

*Розроблено новий метод фільтрації біометричних зображень на основі Атеб-Габора. Метод базується на загальновідомому фільтрі Габора та дозволяє перебудовувати зображення із чіткішими контурами. Тому даний метод має застосування до біометричних зображень, де створення чітких контурів є особливо актуальне. При фільтрації Габором відбувається реконструкція зображення шляхом множення гармонійної функції на функцію Гауса. Атеб-функції є узагальненням елементарної тригонометрії, і, відповідно, володіють більшою функціональністю. Фільтрування Атеб-Габора дозволяє змінювати інтенсивність всього зображення, а також інтенсивність у певних діапазонах, і таким чином зробити певні ділянки зображення контрастнішими. Атеб-функції змінюються від двох раціональних параметрів, а це, в свою чергу, дає можливість гнучкіше керувати фільтрацією. Досліджено властивості Атеб-функції, а також можливості зміни амплітуди функції, частоти коливань на фільтр Атеб-Габора. Показано розв'язання фільтрації на основі двовимірного Атеб-Габора. Ці залежності проаналізовані та зроблені відповідні експерименти. Здійснено визначення співвідношень між частотою та шириною фільтра Атеб-Габора, що дозволило виконувати фільтри для знаходження країв об'єктів з різними частотами та розмірами. Розроблено відповідне програмне забезпечення для фільтрації за допомогою python без використання сторонніх бібліотек, зв'язаних з обробкою зображень. Відбитки пальців відфільтровані за допомогою розробленого фільтра Атеб-Габора. Показано ефективність його використання, яке полягає у більшій кількості варіантів фільтрації опрацьованих зображень. Результати численних експериментів демонструють успішне виділення країв на зображенні на основі отриманих в роботі параметрів фільтра Атеб-Габора*

*Ключові слова: фільтр Габора, Атеб-функції, біометрична система, обробка зображень, відхилення гаусівського ядра*

# DETECTION OF REGULARITIES IN THE PARAMETERS OF THE ATEB-GABOR METHOD FOR BIOMETRIC IMAGE FILTRATION

**M. Nazarkevych**

Doctor of Technical Sciences, Professor\*

E-mail: mar.nazarkevych@gmail.com

**O. Riznyk**

PhD, Associate Professor\*

E-mail: riznykoleg@gmail.com

**V. Samoty**

Doctor of Technical Sciences, Professor

Department of Control and

Information Technologies

Cracow University of Technology

Warszawska str., 24, Cracow, Poland, 31-155

Department of Information Security Management

Lviv State University of Life Safety

Kleparivska str., 35, Lviv, Ukraine, 79003

E-mail: vsamoty@pk.edu.pl

**U. Dzelendzyak**

PhD, Associate Professor\*\*

E-mail: u.dzelendzyak@gmail.com

\*Department of

Publishing Information Technologies\*\*\*

\*\*Department of

Computerized Automation Systems\*\*\*

\*\*\*Lviv Polytechnic National University

S. Bandery str., 12, Lviv, Ukraine, 79013

## 1. Introduction

With the development of information technology, biometrics has widely penetrated into our lives. Biometric identification systems require constant improvement, since they are still very slow and they often produce incorrect results. To date, new methods have been developed for analyzing fingerprints that are scanned contactless. As a result, there are professional systems for recognition. Using the technology of processing "large data", modern systems of monitoring and access control identify individual fragments of biometrics more accurately.

According to the International Biometric Group, the share of fingerprint recognition systems is 52 % of all biometric systems used in the world [1].

In the tasks of recognition, the issue of filtering images is important, since recognition does not always lead to certain

results or means quality. In problems of recognizing biometric data, the software must produce the result at certain intervals [2].

When scanning biometric data, there may be noise on the image that distorts the recognition results. Random noise is manifested in the form of chaotic granularities or extraneous points in the image. Noise is more noticeable in dark areas of images because the signal vs. noise ratio in them is much less than in light areas. Any image received has a number of drawbacks: insufficient sharpness, blurring of the image or indistinctness of some details. Depending on the type of distortion, various image filtration methods that are used in specific situations have been developed to provide different quality of recovery. The use of a filter in one or another situation depends on the type of noise. The most common type is impulse noise. In the case of impact impulse noise

in an image, there are white or black interstices, chaotically scattered over the image. The noise may not be located throughout the image, but the obstacles appear to be isolated contrast points. Today, a large number of noise elimination techniques have been developed. Each individual method is used to eliminate a certain type of noise. The difficulty of finding exact solutions generates different variants of approximate methods.

One of the known methods of filtration is the Gabor filter. It is used for linear filtration and for improving the quality of a converted image. In addition, symmetry, antisymmetry and wavelet transformations can be used to reduce the number of required multiplication and addition operations [3, 4].

However, in a non-processed image, noise can distort lines of imprints, which creates errors in recognition. Besides, identification should be done quickly, within several minutes. For this, the image is improved by applying filtering. This reduces the noise of the image. The Gabor filter based on the *Ateb*-functions is effective for filtration, since it contains a generalization of trigonometric functions [5, 6].

---

## 2. Literature review and problem statement

---

All biometric systems consist of two parts – hardware and specialized software [7]. We will conduct a biometric analysis of the software that helps apply filtering to biometric images.

Modern systems of artificial vision in which the Gabor filtration is used include Skynet, Hunter, DigiNet [8] and the like. In these systems, the quality of the input image plays an important role, and it can be improved by using algorithms based on filtering in frequency or spatial areas, adjusting contrast and brightness. It is very important to use hardware to get a high-quality input image that will change in the process of filtration. Even the above listed systems cannot provide 100 % recognition, so the quality of the filters needs to be improved by creating new and modified ones as well as using multiple filtrations.

Study [9] analyzes the recognition quality and identification properties for 2D Gabor filtration in artificial neural networks. It shows that fingerprint recognition is most effective in recognizing audio signals, veins and biometric characteristics. However, artificial neural networks provide low identification rates. Besides, a drawback of such a method is the need for training in neural networks, which increases the time of recognition of biometric images. Recognition should take a few seconds, and this becomes possible with one-time filtration.

In [10], the Gabor filter is used to filter an audio signal. Filtering is applied repeatedly to achieve the required qualitative results. However, it is noted that recognition by the conventional Gabor filter is not effective. New filters need to be developed to provide identification.

Study [11] shows that qualitative processing of biometric images is achieved with an integrated filtration by the so-called MEA algorithm, which is based on using the Gabor filter, the Laplace filter, and the Volter filter. Gabor filtering allows converting images in frequency and spatial areas. Thus, when applying Gabor filters to fingerprints, the real performance of the structure of the series can be well visible. Changing the settings in the Gabor filter can greatly improve the quality of the input image. Therefore, it is expedi-

ent to use the integrated Laplace filter and Volter filter. This increases the time of processing the image, which is also not desirable in the biometric protection system.

A study has been conducted on the effectiveness of using the Gabor filter among all types of filtration. It was found in [12] that when processing biometric images, the Gabor filter is most often used 3–5 % more frequently than other filters, so it is expedient to expand the filtration options for the specified filter.

In [13], Gabor filtering is considered, and it is shown that in order to make a biometric image suitable for identification, it is necessary to apply self-developed algorithms and to use an anisotropic filtration, which is a lengthy procedure. The time taken to log onto the system should take a few seconds, and additional filtration types increase the time of processing the image, which is unacceptable for a fast logon.

In [14], Gabor filtering is also researched, and it is shown that there are large errors in the scan, which leads to inadequate recognition and identification. When applying Gabor filtering, it is necessary to filter repeatedly and to adjust the angle of inclination, the scale. Therefore, well-chosen options can greatly simplify identification and reduce the time spent in processing an image. This helps find the edges of objects in an image with different frequencies, sizes, and directions.

Studies [15, 16] show that it is necessary to perform identification by a modified Gabor filter in order to achieve high-quality recognition and to ensure a minimum image processing time. For this, it is necessary to develop modified filters based on traditional ones and to provide fast processing time and good-quality identification.

To solve the problem of fingerprint identification, the *Ateb*-Gabor function gives an opportunity to improve the identification process. This provides better characteristics than the traditional Gabor filter. It is proposed to apply a new method of filtration, which is based on the theory of *Ateb*-functions and Gabor filtering. The new filtering method is an extended method of Gabor filtering and ensures small image processing time.

---

## 3. The aim and objectives of the study

---

The aim of the study is to detect the laws of the *Ateb*-Gabor filter, which is based on the use of the mathematical apparatus of the theory of *Ateb*-functions and creates conditions for generating new fast filtering options. The use of the new filter has made it possible to expand filtering sets significantly in order to locate the edges of objects in biometric images successfully.

To achieve the aim, the following objectives are done:

- to find regularities in the properties of one-dimensional and two-dimensional Gabor filters;
- to study the features of *Ateb*-functions for implementing new properties in the *Ateb*-Gabor filter;
- to filter biometric images and to analyze their quality with different sets of *Ateb*-Gabor filters for the successful and quick finding of the edges of objects in biometric images.

---

## 4. Construction of one-dimensional and two-dimensional Gabor filters

---

The formula to construct a one-dimensional Gabor filter [17] is

$$g(z) = e^{(-z^2/2\sigma^2)} \cos(2\Pi\theta z), \quad (1)$$

where  $\sigma$  is the standard deviation of the Gaussian kernel, which determines the amplitude of the function;  $\theta$  is the frequency of alternations, which is defined as  $\theta = 1/T$ , where  $T$  is the period of the function  $\cos(2\Pi\theta z)$ .

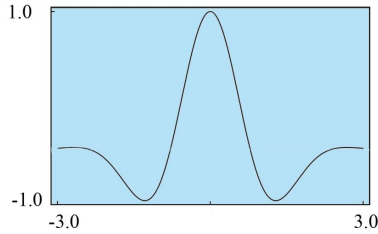


Fig. 1. Construction of a one-dimensional Gabor filter with the parameters of  $\theta=1$  and  $\theta=1$

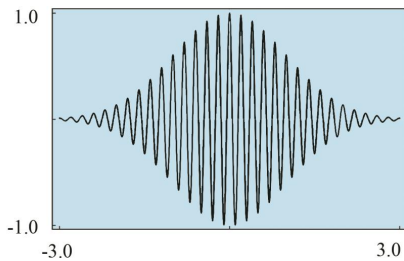


Fig. 2. Construction of a one-dimensional Gabor filter with the parameters of  $\theta=2$  and  $\theta=5$

The bigger the  $\sigma$ , the more declivous the form of the function becomes [18]; the smaller the  $\sigma$ , the acuter the peak of the form of the function (see Fig. 1).

The described index has the properties of a normally distributed random variable. In accordance with the rule of  $3\sigma$ , almost all of its values lie in the interval  $\{-3\sigma; 3\sigma\}$  [12, 19]. For signal processing, these function values are calculated in this segment. Moreover, the higher the value of  $\theta$ , the smaller its period is (Fig. 2).

To filter images, a two-dimensional Gabor filter is used, which is a harmonic function multiplied by the Gaussian function. The two-dimensional Gabor filter looks as follows

$$G(x, y, \lambda, \theta, \psi, \sigma, \varphi) = \exp\left(\frac{-x^2 + \varphi^2 y^2}{2\sigma^2}\right) \cos\left(2\pi \frac{x'}{\lambda} + \psi\right), \quad (2)$$

where

$$\begin{cases} x' = x \cos \theta + y \sin \theta, \\ y' = -x \sin \theta + y \cos \theta. \end{cases}$$

In this equation,  $\lambda$  is the wavelength of the cosine multiplier,  $\theta$  is the frequency of alternations in degrees,  $\zeta$  is the phase shift in degrees, and  $\psi$  is the compression coefficient. Formula (2) is a product of the Gaussian function and the periodic function, and it improves the monotonic regions of periodic fragments in an image [20]. To apply filtration, it is necessary to know the above parameters of the Gabor filter. For fingerprints, it is believed that the frequency of lines and standard deviations are consistent with the local characteristics of the image.

However, the lines of the prints may have different orientations in different parts of the image, so it is necessary

to find the orientation of the lines inside each processed segment. Thus, the modified filter will be a function of three parameters of  $G(x, y, \text{ and } \theta)$ .

The search for the segment orientation is implemented according to the algorithm described by Bazen [21]. The basic idea behind the algorithm is that the gradient of the image corresponding to the fluctuations from white to black will be perpendicular to the lines on the fingerprints. In order that oppositely directed vectors do not compensate each other when averaging, so-called quadrature gradients are calculated [22]. Directions are averaged in each area of the image, and then the corresponding angles of orientation of the fingerprint lines are calculated.

### 5. Construction and properties of *Ateb*-functions for filtration

The mathematical apparatus of the *Ateb*-functions allowed us to solve the analytic systems of differential equations that describe essentially nonlinear processes in systems with one degree of freedom [23].

Let us solve a system of differential equations describing essentially nonlinear processes in systems with one degree of freedom:

$$\begin{cases} \dot{x} + \beta y^m = 0, \\ \dot{y} + \alpha y^m = 0, \end{cases} \quad (3)$$

where  $\alpha$  and  $\beta$  are some real constants, and

$$n = \frac{2\theta'_1 + 1}{2\theta''_1 + 1}, \quad (4)$$

$$m = \frac{2\theta'_2 + 1}{2\theta''_2 + 1}, \quad (\theta'_1, \theta''_1, \theta'_2, \theta''_2 = 0, 1, 2, \dots).$$

Let us consider the case when

$$p = \frac{1}{n+1}, \quad (5)$$

$$q = \frac{1}{m+1},$$

where  $m$  and  $n$  are determined by the formulae of (4).

The *Ateb*-functions are a reversal to the *Beta*-functions. An incomplete *Beta*-function is defined by the equality

$$B_x(p, q) = \int_0^x t^{p-1} (1-t)^{q-1} dt, \quad (6)$$

$$B_1(p, q) = \int_0^1 t^{p-1} (1-t)^{q-1} dt, \quad (7)$$

where  $p$  and  $q$  are some real numbers.

If  $p > 0$  and  $q > 0$ , then the *Beta*-function is definite and continuous, and for other real values of  $p, q$  goes to infinity.

For all  $x$  of the interval  $[0, 1]$ , the functions given by formulae (6) and (7) are positive and satisfy the conditions of [24] that

$$0 \leq B_x(p, q) \leq B_1(p, q),$$

$$B_x(p, q) = B_1(p, q) - B_{-x}(p, q). \tag{8}$$

The *Ateb*-functions developed for the values of (5) are called periodic. System (3), if *m* and *n* satisfy relation (5), describes an oscillatory motion [25].

It is known that *Ateb*-functions are generalizations of ordinary trigonometric functions [25]. A generalization of the Gabor filter based on periodic *Ateb*-functions is proposed. The periodic properties of the *Ateb*-cos required to implement the improved Gabor filter are known and they are described in [26]. The function form is a continuous curve with a period  $T = 2\Pi(m, n)$ .

Intersection with the axis  $\omega$  in the points

$$\left(k + \frac{1}{2}\right) \cdot \Pi(m, n),$$

$k = 0, \pm 1, \pm 2, \dots$  occurs at the angle

$$\gamma = \pm \arctg\left(\frac{2}{m+1}\right).$$

Extremes are achieved at the points  $k\Pi(m, n)$ ,  $k \in \Pi(m, n)$ , and  $k \in Z$  corresponding to  $(-1)^k$ .

The property of periodicity implies that

$$\begin{aligned} Ateb-ca[m, n, \Pi(m, n) + \omega] &= -Ateb-ca(m, n, \omega), \\ Ateb-ca[m, n, 2\Pi(m, n) - \omega] &= -Ateb-ca(m, n, \omega), \\ Ateb-ca[m, n, 2\Pi(m, n) + \omega] &= Ateb-ca(m, n, \omega). \end{aligned} \tag{9}$$

It was also proved in [26] that the introduced *Ateb*-functions are periodic with the period  $2\Pi(m, n)$ , where,

$$2\Pi(m, n) = \frac{\Gamma\left(\frac{1}{n+1}\right) \cdot \Gamma\left(\frac{1}{m+1}\right)}{\Gamma\left(\frac{1}{m+1} + \frac{1}{n+1}\right)}. \tag{10}$$

In formula (10),

$$\Gamma\left(\frac{1}{n+1}\right), \Gamma\left(\frac{1}{m+1}\right), \text{ and } \Gamma\left(\frac{1}{m+1} + \frac{1}{n+1}\right)$$

are the *Gamma*-function.

Properties for the sinus that are used to construct the imaginary component of the Gabor filter are similar.

In (3), the period  $2\Pi(m, n)$  is calculated for various values of *m* and *n* [27], which are given in Table 1.

Table 1

Calculation of the period  $2\Pi(m, n)$  *Ateb-ca*(*m, n*)

<i>M</i>	<i>n</i>	$2\Pi(m, n)$
0.1	1	4.24284
0.5	1	5.17422
1	1	6.28318
2	1	8.41309
3	1	10.4882
4	1	12.5373
5	1	14.5719

The properties for *Ateb-sa*, which are used to construct the imaginary component of the Gabor filter, are similar.

Fig. 3 shows *Ateb-sa* and *Ateb-ca* with the parameters of  $m=1, n=1, \alpha=1$ , and  $\beta=1$ . As can be seen from the graphic map in Fig. 3, it means elementary cosine and sinus. The parameters of  $\alpha=1$  and  $\beta=1$  for (3) are selected in such a way that distortion of the shape of the curves does not occur. Fig. 4 shows *Ateb-ca* and *Ateb-sa* with the parameters of  $m=7, n=7, \alpha=1$ , and  $\beta=1$ . We observe a flat shape of the curves of the function with these parameters, which is well used for filtration. For clarity, Fig. 5 shows a more even form of *Ateb-ca* and *Ateb-sa* with the parameters of  $m=11, n=11, \alpha=1$ , and  $\beta=1$ . Fig. 6 shows *Ateb-ca* and *Ateb-sa* with the parameters of  $m=3, n=3, \alpha=1$ , and  $\beta=1$ . So far, *Ateb-ca* and *Ateb-sa* have been shown with the parameters of  $m=n$ , and with the parameters of  $m \neq n$ , *Ateb-ca* and *Ateb-sa* will not be symmetric, as shown in Fig. 7, where *Ateb-ca* and *Ateb-sa* have the parameters of  $m=5, n=3, \alpha=4$ , and  $\beta=2$ . Fig. 8 demonstrates *Ateb-ca* and *Ateb-sa* with the parameters of  $m=7, n=7, \alpha=4$ , and  $\beta=2$ .

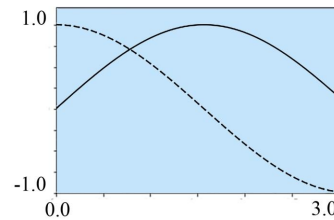


Fig. 3. *Ateb-ca* and *Ateb-sa* with the parameters of  $m=1, n=1, \alpha=1$ , and  $\beta=1$

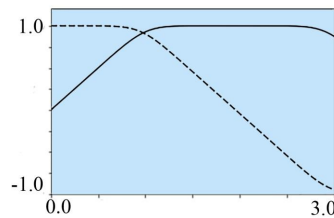


Fig. 4. *Ateb-ca* and *Ateb-sa* with the parameters of  $m=7, n=7, \alpha=1$ , and  $\beta=1$

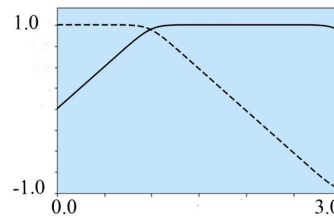


Fig. 5. *Ateb-ca* and *Ateb-sa* with the parameters of  $m=11, n=11, \alpha=1$ , and  $\beta=1$

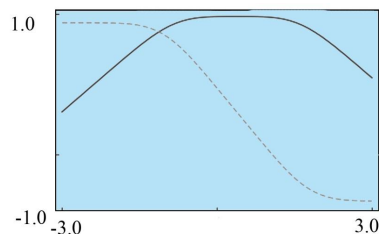


Fig. 6. *Ateb-ca* and *Ateb-sa* with the parameters of  $m=3, n=3, \alpha=1$ , and  $\beta=1$

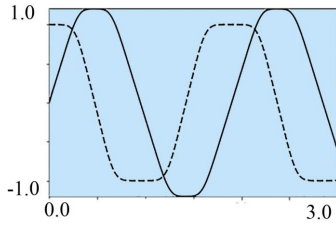


Fig. 7. *Ateb-ca* and *Ateb-sa* with the parameters of  $m=5$ ,  $n=3$ ,  $\alpha=4$ , and  $\beta=2$

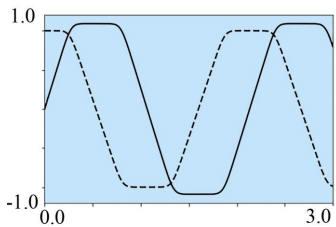


Fig. 8. *Ateb-ca* and *Ateb-sa* with the parameters of  $m=7$ ,  $n=7$ ,  $\alpha=4$ , and  $\beta=2$

The differential equations given in (3) with power nonlinearity are solved. The graphic solutions with various parameters of  $m$  and  $n$  are shown to satisfy the conditions of (4) and (5), and they are periodic. It is shown that solutions of the differential equations with power nonlinearity acquire the values shown in Fig. 3–8. It is noteworthy that this greatly expands the apparatus of trigonometric functions, and therefore we consider it relevant to this study when using image filtration. When applying the mathematical apparatus of the *Ateb*-functions to image filtration, it is possible to increase significantly the control influence on the change of the gradation characteristics of an image.

### 6. Development of one-dimensional and two-dimensional *Ateb*-Gabor filters

Taking into account the above properties of the Gabor filter and the *Ateb*-functions, we construct a generalized one-dimensional Gabor filter based on the *Ateb*-functions. It looks as follows:

$$Ateb-G(m, n, \omega) = \exp\left(-\frac{\omega^2}{2\sigma^2}\right) \cdot Ateb-ca(m, n, 2\Pi, \theta, \omega), \quad (11)$$

where  $\sigma$  is the standard deviation of the Gaussian kernel, which determines the amplitude of the function;  $\omega$  is the frequency of alternations, which is defined as  $\theta = \frac{1}{T}$ , where  $T(m, n)$  is the period of the function *Ateb-ca*( $m, n, 2\Pi, \theta, \omega$ ).

The graphic representation of the generalized Gabor filter is shown in Figs. 9 and 10. Unlike the well-known Gabor filter, the *Ateb*-based filtration has more control actions due to the parameters of  $m$  and  $n$  that can be rational numbers. These control actions will be shown in this study. In the case of  $m = n = 1$ , *Ateb-Gabor* becomes equivalent to the Gabor filter. Since the *Ateb-Gabor* function (*Ateb-G*) is equal and symmetric, the values of *Ateb-G*(1, 0.1) will be identical to *Ateb-G*(0.1, 0).

The *Ateb-Gabor* filter can be used to filter images with a large number of crests. This can provide better characteristics than the well-known Gabor filter. The one-dimensional

Gabor filter based on the *Ateb*-functions makes it possible to obtain more flat shapes, as shown in Fig. 3–6. Thus, filtration with a large spectrum of curves and a larger set of control parameters can be achieved. In particular, the four parameters for the *Ateb*-Gabor filter –  $m$ ,  $n$ ,  $\sigma$ , and  $\theta$ , as opposed to the two –  $\sigma$  and  $\theta$  – for the previously known Gabor filter.

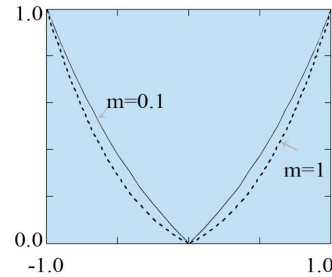


Fig. 9. A graphic representation of *Ateb-G* with the parameters of  $m=0.1$  and  $m=1$  at  $n=1$  and  $\sigma=1$

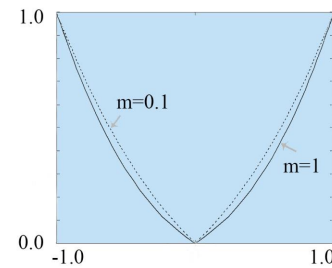


Fig. 10. A graphic representation of *Ateb-G* with the parameters of  $m=0.1$  and  $m=1$  at  $n=1$  and  $\sigma=3$

The two-dimensional *Ateb*-Gabor filtering is performed using the formula

$$Ateb-G(x, y, \lambda, \theta, \psi, \sigma, \xi) = \exp\left(-\frac{x^2 + \psi \cdot y^2}{2\sigma^2}\right) Ateb-ca\left(\frac{2\Pi \cdot x'}{\lambda} + \xi\right). \quad (12)$$

$$\begin{cases} x' = x \cdot \cos(\theta) + y \cdot \sin(\theta), \\ y' = -x \cdot \sin(\theta) + y \cdot \cos(\theta), \end{cases}$$

where  $\lambda$  is the wavelength of the cosine multiplier,  $\theta$  is the orientation of the normal parallel stripes,  $\xi$  is the phase shift, and  $\psi$  is the compression coefficient.

The implementation of such a filter is shown in Fig. 11. It can be noted that if  $m$  and  $n$  are less than 1, the filter will have a shape with many “strokes”. If  $m$  and  $n$  are more than 1, there are usually two black strokes. The filter is made with the parameter of  $\sigma=1$ , the standard deviation of the Gaussian kernel.

The development of filtration based on the two-dimensional *Ateb*-Gabor is shown. Fig. 11 presents filtration by the *Ateb*-Gabor. In particular, the first figure with the parameters of  $m=n=1$  shows the classic Gabor filter. Fig. 12 shows an *Ateb*-Gabor filter with the parameters of  $m=0.2$  and  $n=0.2$  as well as with the angle changes  $\theta=0, \Pi/4, \Pi/2, 3 \Pi/4$  and  $\psi=0, 0.1, 0.2, 0.6$ .

The development of this filter made it possible to increase the number of filtration sets by more than 500 units and to filter the papillary lines’ orientation of fingerprints within a specific area of the image, taking into account the turn and the scale.

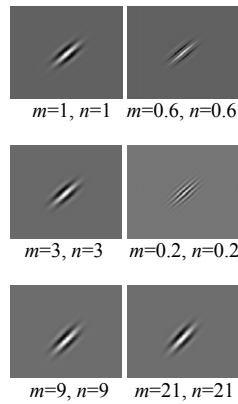


Fig. 11. The *Ateb*-Gabor filter with the parameters of  $m, n$  and  $\sigma=1$

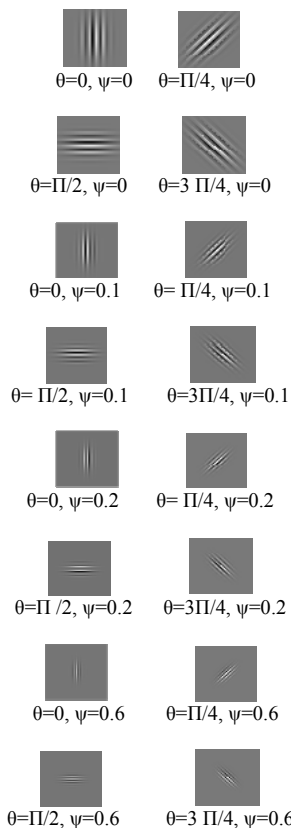


Fig. 12. A graphic representation of *Ateb*-G with the parameters of  $m=0.2$  and  $n=0.2$

### 7. Image processing using the *Ateb*- Gabor filter

Image processing by the *Ateb*-Gabor filter is achieved by averaging the image values in a specific area at each point. The filtration pattern has  $v$  and  $w$  pixels according to the rows and columns, as well as the current pixels and  $i, j$ , which will be changed as a result of the filtering. Accordingly, the use of the *Ateb*-Gabor filter will mean that

$$Ateb-I'(x,y) = \frac{1}{\sigma^2} \sum_{i=1}^n \sum_{j=1}^m I \left( x - \frac{n}{2} + i, y - \frac{m}{2} + j \right) Ateb-G(x,y,\lambda,\theta,\psi,\sigma,\zeta), \quad (13)$$

where  $Ateb-I(x,y)$  is the intensity of the input image at the point  $(x,y)$ ,  $I'(x,y)$  is the intensity of the new image at the

point  $(x,y)$ , and  $G(i,j)$  is the value of the *Ateb*-Gabor function with  $x \in [1,v]$  and  $y \in [1,w]$ .

To use the *Ateb*-Gabor filter, it is necessary to know the following values from formula (12):

- 1) the direction of the filter;
- 2) the frequency of the sinusoidal wave  $\theta$ ;
- 3) the standard deviation of the Gaussian kernel  $\sigma$ .

The frequency response of the filter is determined from the local frequency of  $\omega$  projections, the direction determined by the local orientation. The values of  $\sigma$  are given in the implementation of the algorithm. The bigger these values are, the more noise-proof the filter will be. However, more distortions will be introduced, creating non-existent projections and depressions. If the values of  $\sigma$  are chosen to be low, the filter will not distort, but its filtering ability will decrease. This will result in ineffective noise removal. Therefore, when selecting the values, it is advisable to find a compromise between the efficiency of the filter and the absence of distortions made by the filter. As a rule, these parameters are chosen empirically [28].

In the study of papillary lines of fingers, there are such features as described in [29, 30]. For each fingerprint, it is possible to determine two types of attributes – global and local [31]. Global signs can be seen with the naked eye. Local signs are the features of the direction of the papillary lines that are unique for each imprint [32, 33]. The distinction is due to the fact that the lines of fingerprints are not straight-forward. They are often broken, branched, change direction and have gaps. The points in which the lines end, branch, or change the direction are called minutiae [33]. These points provide unique fingerprint information when identifying a person. Each fingerprint contains up to 70 minutiae [33].

The relationship between the frequency and the width of the *Ateb*-Gabor filter has been determined, which allows the filters to automatically find the edges of objects with different frequencies, sizes, and directions. A method is proposed for removing the average component of the *Ateb*-Gabor filter, which helps reduce the average filter value to zero without deforming the filter. The results of numerous experiments demonstrate the successful selection of edges in an image based on the parameters of the *Ateb*-Gabor filter.

Below is a snippet of the code that calculates the value of *Ateb*-functions. Numerous methods for calculating *Ateb-ca* were used in papers [25–27]. In this study, *odeint* was used from the *Python scipy* library. The results of the *Ateb*-Gabor filter, which filters fingerprints, are shown in Fig. 13.

```
#calculating of the Ateb-functions
#based on the solution of the differential equation

alpha = -1
beta = 1

n = 1
m = 1
P = period(m, n)
num = 100000;
def model(z,t):
    dxdt = -alpha* z[1]**n #pow(z[1],n)
    dydt = -beta*z[0]**m
    dzdt = [dxdt,dydt]
    return dzdt
```

```
# initial condition
z0 = [0,1]

# time points
t = np.linspace(0,P, num)

# solve ODE
z = odeint(model,z0,t)
#z consistst of the ca values
```

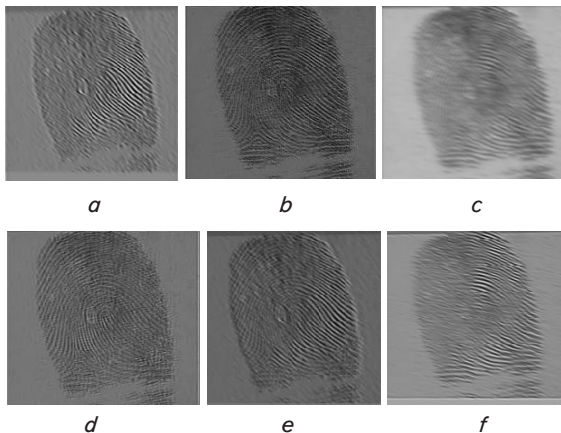


Fig. 13. The results of *Ateb-Gabor* filtering with various parameters: *a* –  $m=1.2, n=5$ , *b* –  $m=11, n=11$ , *c* –  $m=41, n=41$ , *d* –  $m=3, n=3$ , *e* –  $m=7, n=7$ , *f* –  $m=1, n=1$

Fig. 13 shows *Ateb-Gabor* filtration with different parameters of  $m$  and  $n$ . In conducting the study, we can specify that  $m=n=3$  and  $m=n=7$  give the best results of filtration.

The filter results shown in Fig. 13 are executed in Python 3 without the use of third-party libraries that are associated with image processing. The software is a prototype of the working version without optimizing the algorithm over the program time. The algorithm can be accelerated by using scheduling in the Fourier series when performing a convolutional operation, as well as by parallel processing of individual segments of an image.

### 8. Discussion of the results of researching the effectiveness of the new *Ateb-Gabor* filter

It is shown that the new *Ateb-Gabor* filter has a much greater functionality, since it is based on a new mathematical apparatus that extends elementary trigonometric functions. This increases the number of options for using modified images. Thus, the new filtering method will allow identification in biometric images and provide better quality metrics. This will make it possible to use filtration once, avoiding multiple filtrations, which reduces the time of processing biometric images.

The research has revealed the regularities in the properties of a one-dimensional *Ateb-Gabor* filter, which consist in the introduction of rational parameters of  $m$  and  $n$  as well as the use of the periodic *Ateb*-function, which is an advantage of the developed method of filtration.

The study has implemented a method for generating new fast filtering options that are based on the expansion of filtration sets, which makes it possible to find the edges of objects in biometric images and, as a result, perform the identification and recognition of biometric images more effectively.

The research findings can be used to recognize biometric images. The application of the new *Ateb-Gabor* filter allows filtering to be made taking into account the turn and extent of the papillary lines of a finger in a specific area of an image. The study was carried out for filtration with the parameters of  $m=n$ ; it still remains to consider filtration when  $m \neq n$  and the impact on biometric images in such a case.

A disadvantage is that the complexity of the *Ateb-Gabor* filtering algorithm has not been calculated. Besides, there have been neither timed filtering tests on the developed filter nor comparisons with filtering time by the traditional Gabor filter. Such tests require high resource costs and can be developed in new studies. The unresolved issues are the development of the search for effective algorithms for changing the direction of orientation of the *Ateb-Gabor* filter relative to the direction of the papillary lines of a biometric image to construct the vector image format.

The development of this study is considered to be a correction of these shortcomings, after which the *Ateb-Gabor* filter will become versatile and justifiable as to the recommendations for its usage.

This study is useful in constructing biometric image recognition systems, which have recently been rapidly developed and are important. In the future, it is planned to analyze images when filtering with the parameters of *Ateb-Gabor* where  $m \neq n$  and perform the identification.

### 9. Conclusion

1. The study has revealed patterns in the properties of the *Ateb-Gabor* filter. They consist in the fact that this filter is based on the mathematical apparatus of *Ateb*-functions and the Gabor function. The *Ateb*-functions help obtain the values of solutions of differential equations with power nonlinearity and depend on two rational parameters –  $m$  and  $n$ . Due to these parameters, the *Ateb-Gabor* filter acquires new features in filtering. Changing the  $m$  and  $n$  parameters provides new values for the *Ateb-Gabor* period, which makes it possible to extend the number of filtering sets. This allows one-time filtration, avoiding multiple filtering, which significantly reduces the time of processing a biometric image.

2. The properties of *Ateb*-functions were constructed and investigated. It has been specified that *Ateb*-functions are a generalization of trigonometric functions. The period of *Ateb*-functions was calculated for the periodic function. The patterns in one-dimensional and two-dimensional *Ateb-Gabor* filters have been revealed. The *Ateb-Gabor* filtering helps get more flat shapes and significantly increase the number of filtering sets. The development of this filter has made it possible to increase the number of filtration sets to more than 500 units. Two-dimensional filtering by the *Ateb-Gabor* filter was performed taking into account the orientation of the turn and the scale of the finger papillary lines in a specific area of an image.

3. The correlation between the frequency and width of the *Ateb-Gabor* filter has been determined, which makes it possible to filter in order to find the edges of objects with different frequencies, sizes, and directions. The results of numerous experiments demonstrate a successful selection of edges in an image based on the parameters of the *Ateb-Gabor* filter.

## References

1. Biometrics Market and Industry Report 2009–2014 // International Biometric Group. 2007.
2. Handbook of Fingerprint Recognition / Maltoni D., Maio D., Jain A. K., Prabhakar S. Springer, 2009. 494 p. doi: <https://doi.org/10.1007/978-1-84882-254-2>
3. Lee T. S. Image representation using 2D Gabor wavelets // IEEE Transactions on Pattern Analysis and Machine Intelligence. 1996. Vol. 18, Issue 10. P. 959–971. doi: <https://doi.org/10.1109/34.541406>
4. Sebe N. Image retrieval using wavelet-based salient points // Journal of Electronic Imaging. 2001. Vol. 10, Issue 4. P. 835. doi: <https://doi.org/10.1117/1.1406945>
5. Data protection based on encryption using Ateb-functions / Nazarkevych M., Oliarnyk R., Troyan O., Nazarkevych H. // 2016 XIth International Scientific and Technical Conference Computer Sciences and Information Technologies (CSIT). 2016. doi: <https://doi.org/10.1109/stc-csit.2016.7589861>
6. Senik P. M. Inversion of the incomplete beta function // Ukrainian Mathematical Journal. 1970. Vol. 21, Issue 3. P. 271–278. doi: <https://doi.org/10.1007/bf01085368>
7. Sree Vidya B., Chandra E. Multimodal biometric hashkey cryptography based authentication and encryption for advanced security in cloud // Biomedical Research. 2018. doi: <https://doi.org/10.4066/biomedicalresearch.29-17-1766>
8. Russell S. J., Norvig P. Artificial intelligence: a modern approach. Malaysia; Pearson Education Limited, 2016.
9. Meitram R., Choudhary P. Palm Vein Recognition Based on 2D Gabor Filter and Artificial Neural Network // Journal of Advances in Information Technology. 2018. Vol. 9, Issue 3. P. 68–72. doi: <https://doi.org/10.12720/jait.9.3.68-72>
10. Akin C., Kacar U., Kirci M. A Multi-Biometrics for Twins Identification Based Speech and Ear // arXiv. 2018. URL: <https://arxiv.org/ftp/arxiv/papers/1801/1801.09056.pdf>
11. Arif A., Li T., Cheng C.-H. Blurred fingerprint image enhancement: algorithm analysis and performance evaluation // Signal, Image and Video Processing. 2017. Vol. 12, Issue 4. P. 767–774. doi: <https://doi.org/10.1007/s11760-017-1218-0>
12. Andrew A. M. Handbook of fingerprint recognition, by Davide Maltoni, Dario Maio, Anil K. Jain and Salil Prabhakar, Springer, New York, 2003, hardback, xii + 348 pp., with DVD-ROM, ISBN 0-387-95431-7 ( 46.00) // Robotica. 2004. Vol. 22, Issue 5. P. 587–588. doi: <https://doi.org/10.1017/s026357470422094x>
13. Gottschlich C. Curved-Region-Based Ridge Frequency Estimation and Curved Gabor Filters for Fingerprint Image Enhancement // IEEE Transactions on Image Processing. 2012. Vol. 21, Issue 4. P. 2220–2227. doi: <https://doi.org/10.1109/tip.2011.2170696>
14. Gopi K. Fingerprint Recognition Using Gabor Filter And Frequency Domain Filtering // IOSR Journal of Electronics and Communication Engineering. 2012. Vol. 2, Issue 6. P. 17–21. doi: <https://doi.org/10.9790/2834-0261721>
15. Adaptive Fingerprint Image Enhancement With Emphasis on Preprocessing of Data / Bartunek J. S., Nilsson M., Sallberg B., Claesson I. // IEEE Transactions on Image Processing. 2013. Vol. 22, Issue 2. P. 644–656. doi: <https://doi.org/10.1109/tip.2012.2220373>
16. Orthogonal curved-line Gabor filter for fast fingerprint enhancement / Mei Y., Chen S., Zhou Y., Zhao B. // Electronics Letters. 2014. Vol. 50, Issue 3. P. 175–177. doi: <https://doi.org/10.1049/el.2013.2619>
17. Kassis M., El-Sana J. Scribble Based Interactive Page Layout Segmentation Using Gabor Filter // 2016 15th International Conference on Frontiers in Handwriting Recognition (ICFHR). 2016. doi: <https://doi.org/10.1109/icfhr.2016.0016>
18. Jones J. P., Palmer L. A. An evaluation of the two-dimensional Gabor filter model of simple receptive fields in cat striate cortex // Journal of Neurophysiology. 1987. Vol. 58, Issue 6. P. 1233–1258. doi: <https://doi.org/10.1152/jn.1987.58.6.1233>
19. Grigorescu S. E., Petkov N., Kruizinga P. Comparison of texture features based on Gabor filters // IEEE Transactions on Image Processing. 2002. Vol. 11, Issue 10. P. 1160–1167. doi: <https://doi.org/10.1109/tip.2002.804262>
20. Ali M. A. M., Tahir N. M. Half iris Gabor based iris recognition // 2014 IEEE 10th International Colloquium on Signal Processing and its Applications. 2014. doi: <https://doi.org/10.1109/cspa.2014.6805765>
21. Bazen A. M., Gerez S. H. Fingerprint matching by thin-plate spline modelling of elastic deformations // Pattern Recognition. 2003. Vol. 36, Issue 8. P. 1859–1867. doi: [https://doi.org/10.1016/s0031-3203\(03\)00036-0](https://doi.org/10.1016/s0031-3203(03)00036-0)
22. Petrovic V. S., Xydeas C. S. Gradient-Based Multiresolution Image Fusion // IEEE Transactions on Image Processing. 2004. Vol. 13, Issue 2. P. 228–237. di: <https://doi.org/10.1109/tip.2004.823821>
23. Struble R. A. Nonlinear differential equations. Courier Dover Publications, 2018. 288 p.
24. Senik P. M., Vozniy A. M. Chislennoe obrashchenie odnogo klassa nepolnoy Beta-funkcii // Matematicheskaya fizika. 1973. Issue 14. P. 160–164.
25. Gricik V. V., Nazarkevich M. A. Mathematical models algorithms and computation of Ateb-functions // Dopovidi NAN Ukraini Seriji A. 2007. Issue 12. P. 37–43.
26. Nazarkevych M., Hladets A. Development of software package for the encryption of electronic documents means Ateb-functions // Bulletin of the Lviv Polytechnic National University, Computer Science and Information Technology. 2009. Issue 638. P. 55–61.
27. The method of encryption based on Ateb-functions / Nazarkevych M., Oliarnyk R., Nazarkevych H., Kramarenko O., Onyshchenko I. // 2016 IEEE First International Conference on Data Stream Mining & Processing (DSMP). 2016. doi: <https://doi.org/10.1109/dsmp.2016.7583523>
28. Handbook of fingerprint recognition / Maltoni D., Maio D., Jain A. K., Prabhakar S. Springer, 2009. doi: <https://doi.org/10.1007/978-1-84882-254-2>
29. Handbook of Fingerprint Recognition / Maltoni D., Maio D., Jain A. K., Prabhakar S. Springer, 2003.



30. Fingerprint matching using minutiae and texture features // Proceedings 2001 International Conference on Image Processing (Cat. No.01CH37205). 2002. doi: <https://doi.org/10.1109/icip.2001.958106>
31. Impact of artificial «gummy» fingers on fingerprint systems / Matsumoto T., Matsumoto H., Yamada K., Hoshino S. // Optical Security and Counterfeit Deterrence Techniques IV. 2002. doi: <https://doi.org/10.1117/12.462719>
32. Model of stegosystem images on the basis of pseudonoise codes / Riznik O., Yurchak I., Vdovenko E., Korzhagina A. // In Perspective Technologies and Methods in MEMS Design (MEMSTECH), 2010 Proceedings of VIth International Conference. 2010.
33. Fries M., Fischbach R., Houdeau D. U.S. Pat. No. 6.347.040. Washington, DC: U.S. Patent and Trademark Office, 2002.

*Запропоновано метод виявлення шахрайства при інсталюванні мобільних додатків. Розроблений метод на відміну від існуючих використовує всі наявні дані, незалежно від типів, розмірності і розбіжності цих даних та перетворює такі дані до однорідних коефіцієнтів на основі запропонованого методу шкалювання. Такий підхід дозволяє підвищити точність розв'язання задачі та побудувати відкриту до розширення базу знань з характеристиками шахраїв та правилами виявлення користувачів-шахраїв. Розроблена система шкал для перекладу різнорідних даних до однорідних коефіцієнтів, яка дозволила побудувати математичну модель процесу шкалювання. Розроблено алгоритм шкалювання різнорідних масивів даних на основі запропонованих шкал та математичної моделі процесу шкалювання великих масивів різнорідних даних, що дозволило всю множини даних привести до двох однорідних груп. Запропоновано алгоритми обробки отриманих груп однорідних даних та виявлення користувачів-шахраїв. Розроблені алгоритми з використанням коефіцієнтів схожості між характеристиками користувачів формують шаблони шахраїв, визначають характеристики та залежності користувачів-шахраїв, що дозволяє підвищити ефективність та швидкість процесу виявлення шахраїв. Була запропонована схема процесу виявлення шахраїв, що використана в інтелектуальній системі автоматичного виявлення шахраїв для проведення експериментальних досліджень. За результатами експериментальних досліджень отримана точність визначення шахраїв на заданій репрезентативній вибірці 99,14 %. Результати експериментальних досліджень показали ефективність автоматичного виявлення шахраїв та можливість розширення форматів та характеристик користувачів-шахраїв на основі інтелектуального аналізу і баз знань*

*Ключові слова: виявлення шахрайства, різнорідні дані, інсталювання мобільних додатків, аномалії в даних, шкалювання даних*

UDC 004.8:044.89

DOI: 10.15587/1729-4061.2019.155060

## DEVELOPMENT OF A METHOD FOR FRAUD DETECTION IN HETEROGENEOUS DATA DURING INSTALLATION OF MOBILE APPLICATIONS

T. Polhul

Postgraduate student\*

E-mail: tanapolg93@gmail.com

A. Yarovyj

Doctor of Technical Sciences,  
Professor, Head of Department\*

E-mail: a.yarovyy@vntu.edu.ua

\*Department of Computer Science  
Vinnytsia National Technical University  
Khmelnytske shose str., 95,  
Vinnytsia, Ukraine, 21021

### 1. Introduction

Promotion of mobile software is typical for the present-day IT market. For such activity, companies should spend a lot of money on marketing campaigns. One of the options of determining effectiveness of a marketing campaign consists in checking the number of mobile app installations provided by the company. It is worth to know at this step that a certain part or entire set of mobile app installations could be performed in a fraudulent way. Knowing the actual number of organic mobile app installations and the number of fraudulent installations, one can determine real cost of a marketing campaign and whether it is effective. Note that fraudulent users are called fraudsters. Therefore, develop-

ment of a system for automatic detection of fraudsters and marketing campaigns using fraudulent methods of installation is a relevant task in this field.

### 2. Literature review and problem statement

Complexity of the problem that arises in this study consists first and foremost in uncertainty of the “fraud” concept in technical literature. For example, fraud is considered in [1] as a some sort of anomalies in data. In its turn, anomaly can be defined as contextual (conditional) anomaly “if a copy of data is abnormal in a particular context.” Methodology for detecting this type of anomaly “takes into account